The photoelectron bandstructure of molybdenum disulphide

The photoelectron bandstructure of molybdenum disulphide

K Fives†, I T McGovern†, R McGrath‡, R Cimino§, G Hughes||, A McKinley¶ and G Thornton††

† Department of Pure and Applied Physics, Trinity College, Dublin 2, Ireland
‡ Interdisciplinary Research Centre in Surface Science and Department of Physics, Liverpool University, PO Box 147, Liverpool L69 3BX, UK
§ Fritz-Haber-Institut der MPG, Faradayweg, Berlin 33, Federal Republic of Germany
|| Department of Physics, Dublin City University, Dublin 11, Ireland
¶ Department of Applied Physical Sciences, University of Ulster, Coleraine, Northern Ireland
†† Interdisciplinary Research Centre in Surface Science and Department of Chemistry, University of Manchester, Manchester M13 9PL, UK

Abstract. An experimental electronic bandstructure of molybdenum disulphide has been determined from angle-resolved ultraviolet photoelectron spectroscopy (ARUPS) measurements: polar-angle-dependent ARUPS at a photon energy of 21.2 eV allows us to obtain an approximate plot of dispersion parallel to the basal face while photon-energy-dependent ARUPS at normal emission gives a plot of dispersion perpendicular to this face. The experimental bandstructure is compared with three calculations and, while there is a general agreement, specific aspects are better reproduced when there is self-consistency in the calculations. An analysis difficulty reported earlier for polar angle ARUPS for this material can now be understood as arising from incorrect labelling of symmetry directions in the experiment.

1. Introduction

The layer-lattice solids have a unique atomic structure in which bonding within a layer is strong while that between layers is very weak (Wilson and Yoffe 1969). The resultant quasi-two-dimensional electronic structure of layer-lattice solids was exploited in the early development of the technique of angle-resolved ultraviolet photoelectron spectroscopy (ARUPS). Photoelectron momentum is only conserved for the component parallel to the surface; to a first approximation the layer-lattice solid has no dispersion perpendicular to the basal surface and hence the so-called 'k-parallel' or $E(k_{||})$ plot in polar-angle-dependent ARUPS is a reasonable measure of the two-dimensional, electronic bandstructure (Hughes and Liang 1973).

A number of layer-lattice materials have been studied by this technique (Smith and Traum 1975, Lloyd *et al* 1976). However, an early $E(k_{||})$ investigation of molybdenum disulphide (McGovern *et al* 1979) did not show much agreement with the available calculated bandstructures; the complexity of the bandstructure was cited as a possible explanation. Recently, however, Coehoorn *et al* (1987) demonstrated that there was no difficulty in matching ARUPS-derived electronic structure with bandstructure calculations for the related material MoSe$_2$, and Mamy *et al* (1987) showed that this

was also the case for MoS_2. The first theme of this paper is the presentation of a synopsis of the results of a remeasurement of $E(k_\parallel)$ for this material. These results are very similar to those of Mamy *et al* (1987) and hence only the dispersion plots are included. These are presented in order to make comparison with calculations other than those in Mamy *et al* (1987) and to show how the earlier difficulty in interpretation (McGovern *et al* 1979) is due to an experimental error.

The second theme of this paper is to present recent 'k-perpendicular' or $E(k_\perp)$ ARUPS measurements of MoS_2. These data probe the bandstructure in the third dimension, i.e. normal to the layers, using the tunable photon energy of synchrotron radiation. This corresponds to the ΓA direction in the bulk Brillouin zone. Mapping the bandstructure along ΓA allows us to assess critically the assumption that the $E(k_\parallel)$ data can be equated with dispersion parallel to the basal surface. The measurements also illustrate selection rule effects associated with the non-symmorphic space group of $2H-MoS_2$.

2. Experimental details

The ARUPS measurements were performed in two separate ADES 400 spectrometers. In one case the photon source was a helium discharge lamp with photon energy equal to 21.2 eV (He I); the polar angle dependence of spectra provided the $E(k_\parallel)$ plot. In the other case the source was the monochromatized continuum of synchrotron radiation. Initial measurements of this latter type were performed on the Beamline 6 toroidal grating monochromator (TGM) at SRS, Daresbury Laboratory, while a more complete dataset was obtained on the TGM2 beamline at BESSY in Berlin; the photon energy dependence of spectra at normal emission provided the $E(k_\perp)$ plot. In the synchrotron radiation measurements the combined analyser and photon energy resolution was better than 250 meV throughout the photon energy range 25–60 eV; in the He I measurements the analyser resolution was $\simeq 200$ meV. In both cases the angular resolution was $\pm 2°$.

Basal faces of molybdenum disulphide were prepared by *in situ* cleaving of natural molybdenite crystals in vacua better than 10^{-8} mbar. This pressure allows ample time for measurements on these very inert surfaces. Azimuthal orientation was checked by LEED. The two principal directions within the surface plane are associated with the azimuthal planes ΓALM and ΓAHK of the Brillouin zone; the surface projection of the ΓALM plane has reflection symmetry at the zone edge in the repeated-zone scheme. The direction normal to the surface plane is ΓA in the Brillouin zone. The full three-dimensional zone for $2H-MoS_2$ is shown in figure 1(a).

The ARUPS geometry for the polar angle measurements is shown in figure 1(b). The light was incident at 45° with respect to the surface normal and the polar angle of electron emission was in the plane of incidence. The emission angle θ_e is negative in the quadrant containing the incident light, where it is limited to $-30°$. The projection of the emission vector onto the surface gives the emission azimuth (either ΓALM or ΓAHK, as above). For the normal emission data the light was also incident at 45° with respect to the surface normal; the plane of incidence was aligned with the azimuth ΓAHK and the light was plane polarized in this plane of incidence.

3. Results

Experimental $E(k_\parallel)$ plots for the ΓALM and ΓAHK azimuths are shown in figure 2.
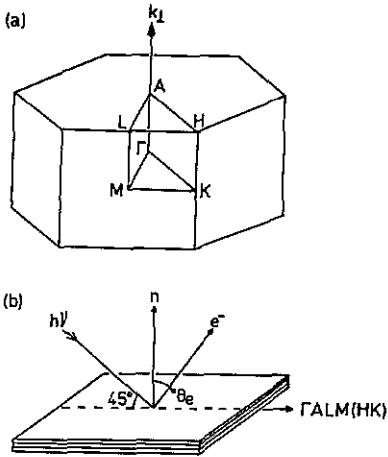
(a)

(b)

Figure 1. (a) The Brillouin zone for 2H-MoS₂; (b) schematic diagram of the ARUPS geometry.
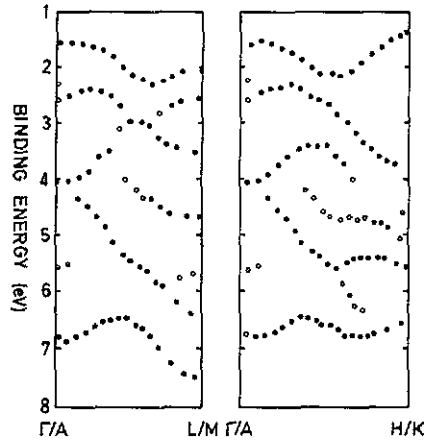
Figure 2. The experimental $E(k_{\parallel})$ dispersion for the ΓALM and ΓAHK azimuths, following zero-angle correction and symmetrization at the L/M point.

Following Hughes and Liang (1973), these plots were obtained by the usual procedure of determining the kinetic energy relative to the vacuum level (E_k) of each peak in the spectrum at a particular emission angle (θ_e) and computing the corresponding value of $k_{\parallel}$ from the free-electron relation

$$k_{\parallel} = 0.51\sqrt{E_k}\,\sin\theta_e. \tag{1}$$

This yields a series of points with coordinates (E_k, $k_{\parallel}$). The mesh employed for θ_e was 2.5° between −30° and +35° and 5° between +40° and +75°, giving a somewhat larger dataset than Mamy *et al* (1987). The reflection symmetry of positive and negative θ_e allowed an accurate determination of the sample normal direction. A second reflection symmetry in the ΓALM dataset provided a good estimation of the zone edge. This resulted in an experimental value for the zone distance AL/ΓM of 1.12 Å⁻¹ which compares well with the calculated structure value of 1.145 Å⁻¹. The experimental zone distance AH/ΓM was calculated from the experimental value for AL/ΓM. The experimental plots in figure 2 are shown in the more usual form of binding energy relative to the Fermi level; the full and empty circles are data points derived from peaks and shoulders, respectively.

Normal-emission, variable-photon-energy spectra are presented in figure 3; the mesh in photon energy was 1 eV. Following Chiang *et al* (1980), these data were analysed using the expression

$$k_{\perp} = 0.51\sqrt{E_k + V_0} \tag{2}$$

where V_0 is the magnitude of the inner potential, relative to the vacuum level. The value of V_0 was varied to give the best fit to the symmetry of the repeat distance of the zone. This symmetry occurs at *twice* the ΓA distance because of dipole selection rules for the non-symmorphic space group of 2H-MoS₂ (Coehoorn *et al* 1987). The best fit was obtained for $V_0 = 8$ eV and the resultant $E(k_{\perp})$ plot of binding energy
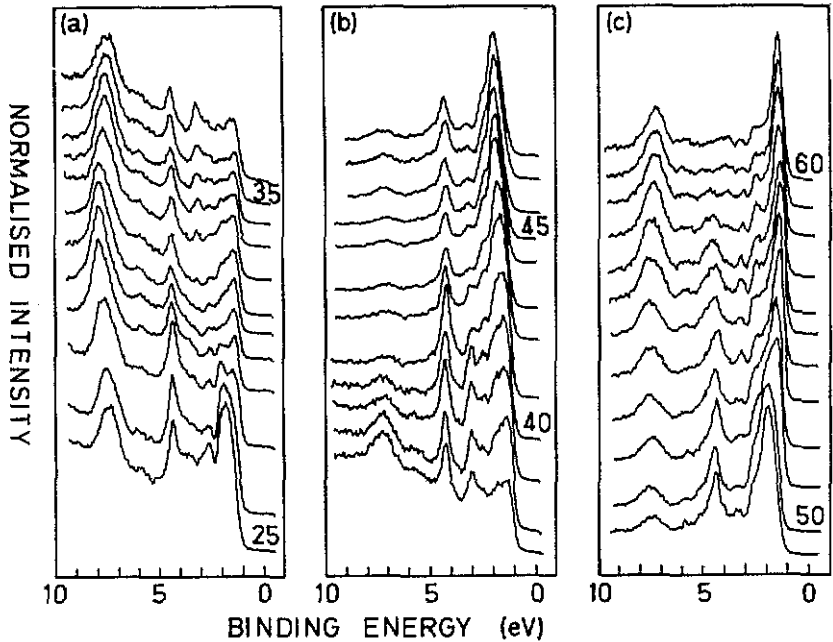
Figure 3. Normal-emission ARUPS spectra in the photon energy ranges (a) 25–36 eV, (b) 37–48 eV and (c) 49–60 eV.

relative to the Fermi level is shown in figure 4(a). This value of V_0 lies within the range 5 to 10 eV suggested by LEED investigations (Mrstik *et al* 1977, Williams *et al* 1971).

It is apparent that the major dispersion is in the top and bottom bands in figure 4(a). The large scatter in the data and the lower overall $E(k_\perp)$ dispersion make it difficult to determine accurately the reflection symmetry condition that occurs at around 2.5 Å^{-1} and 3.5 Å^{-1}. The final $\Gamma A \Gamma$ $E(k_\perp)$ plot shown in figure 4(b) is obtained by back-folding the data in figure 4(a) at about 3.0 Å^{-1}. This operation increases the scatter in the data.

4. Discussion

In this section the experimental plots of figures 3 and 4 are compared with the bandstructures reproduced from three separate calculations. These are the tight-binding (TB) method of Bullett (1978), the layer-scattering (LS) method of Doran (1980) and the augmented spherical wave (ASW) method of Coehoorn *et al* (1987).

In principle, the experimental $E(k_{\parallel})$ dispersion does not correspond to any symmetry direction of the calculations, but rather to a complex path within the corresponding azimuthal plane of the zone. It is common practice (see, e.g., Cochoorn *et al* 1987) to show the experimental points against the doubled bandstructure of the mid-zone plane, along ΓM, say. This certainly covers the extrema of possible dispersion but the diagram is often so cluttered that the comparison with experiment is limited. We have adopted the alternative approach of showing the simpler degenerate bandstructure of the zone top, along AL, say. We believe that this will also provide a reasonable representation of the $E(k_{\parallel})$ dispersion if the dispersion in $k_\perp$ is not too
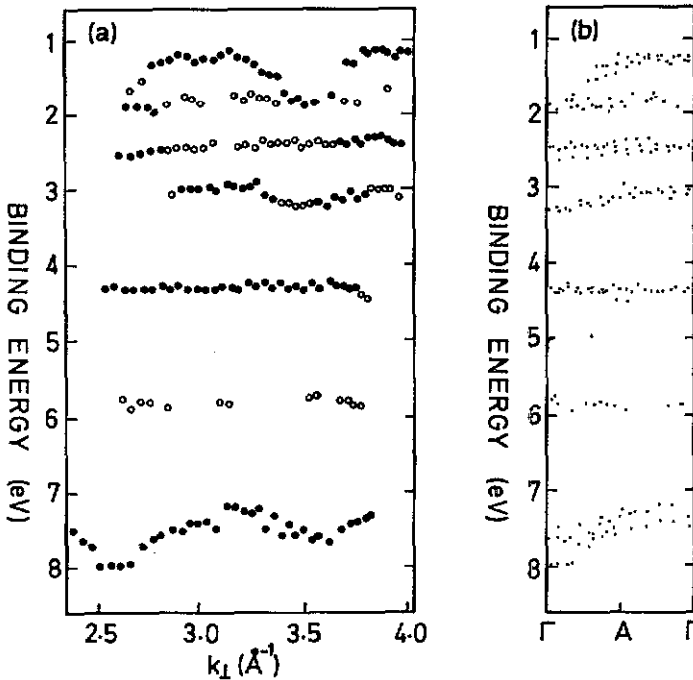
Figure 4. (a) The experimental $E(k_\perp)$ dispersion derived from the spectra of figure 3, using $V_0 = 8$ eV; (b) the experimental $E(k_\perp)$ dispersion after the back-folding operation.

large. A further consideration is that one of the calculations (TB) provides only this zone-top dispersion, i.e. along AL and AH.

The AL and AH bandstructures redrawn from the TB, LS and ASW calculations are compared with the experimental $E(k_\parallel)$ dispersions in figure 5. The panels are arbitrarily aligned using the doubly degenerate A point at around 4 eV binding energy. The general features of the experimental $E(k_\parallel)$ dispersion are reproduced in all three calculated bandstructures. In the discussion of the earlier measurements (McGovern *et al* 1979), it was suggested that the complexity of the molybdenum disulphide bandstructure and that of the emission process were reasons for the then poor agreement between experiment and calculation: it is clear from the present results (also from the data of Mamy *et al* (1987)) that there are no such difficulties for this material; the reason for the lack of agreement lies with the measurements. There are two aspects here: first, a rather large mesh of 5° and a tendency for overall binding energy to drift to higher values at larger polar angles (an analyser problem) made it difficult to locate the reflection symmetry in the ΓALM dataset. This contributed to the second and more serious aspect which is that it would appear that the AL and AH directions have been mistakenly reversed in the earlier data. As shown in figure 2, a clear signature of the AL direction is the 'scissors' shape formed by the second- and third-highest bands; in the earlier paper this shape is more apparent in the experimental $E(k_\parallel)$ dispersion labelled ΓK, which is equivalent to AH in the notation used here.

In the general scheme for the electronic structure of MoS_2, the top band has Mo 4d character (the d_{z^2} band) while the remaining bands have largely S 3p character
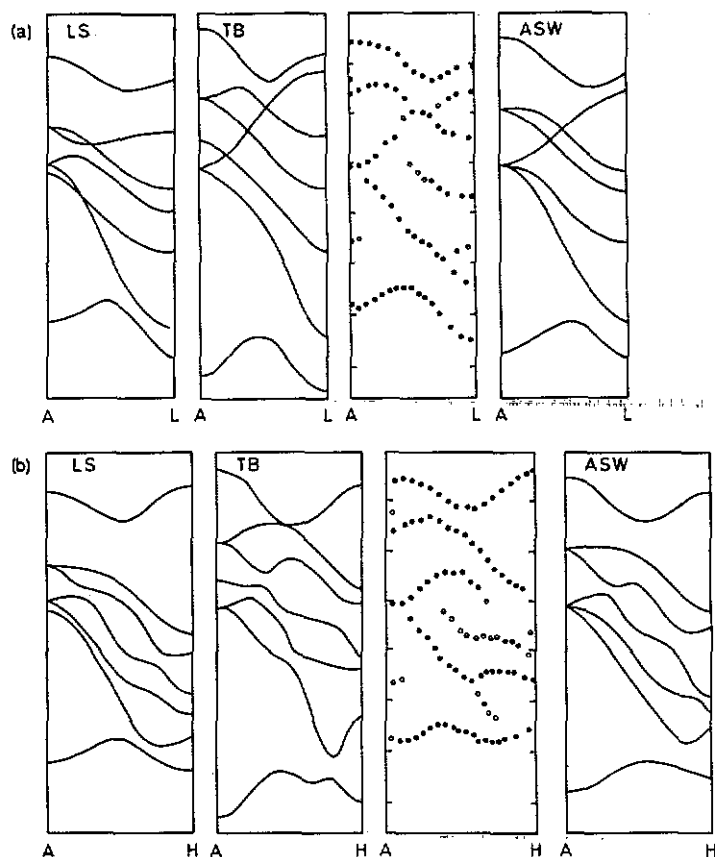
Figure 5. The comparison of the experimental $E(k_\parallel)$ dispersion from figure 2 with the calculated bandstructures (a) along AL and (b) along AH. The calculations are labelled LS (Doran 1980), TB (Bullett 1978) and ASW (Coehoorn *et al* 1987).

(Doran 1980). Although recent resonant photoelectron spectroscopy measurements show that the upper half of this 'p band' also has significant 4d character (Lince *et al* 1991), it is helpful to use the simpler description. Given that the top band has some $E(k_\perp)$ dispersion, as shown in figure 3, the experimental $E(k_\parallel)$ dispersion of the d band for both symmetry directions is well reproduced in all three calculations. With the same consideration of $E(k_\perp)$ dispersion applying to the bottom band, the general agreement is again quite good. The lack of $E(k_\perp)$ dispersion for the remaining p bands make these a better test of the detailed differences in the calculations.

It is clear that the TB calculation overestimates the overall width of the valence band. However, this calculation replicates the shape of the upper p bands and, more importantly, provides a much better measure of the d to p separation than that of the LS calculation. One difference between these two calculations is that the TB method attempts some measure of self-consistency by employing a $d^{4.7}$ configuration derived from the Mo–S electronegativity difference. The generally self-consistent ASW calculation may be judged to provide the best overall agreement. It does depart from self-consistency in its treatment of the non-metal polarizability; this is effectively achieved by varying the crystal parameter z, where zc is the distance between the metal and non-metal atom layers (c is the lattice constant perpendicular to the layers).

The value of z used in this calculation for MoS$_2$ was the same as that obtained from the best fit between experiment and calculation for the related material MoSe$_2$.

The experimental $E(k_\perp)$ dispersion is compared with the $\Gamma A \Gamma$ unfolded zone bandstructures of the three calculations in figure 6. The unfolding was achieved by following the selection rule analysis outlined by Coehoorn *et al* (1987). Of the seven bands, which are labelled 1 to 7 with increasing binding energy, bands 1, 4, 5 and 7 correspond to well defined spectral features. The experimental and calculational panels are arbitrarily aligned so that band 5 coincides with the deeper of the two fairly flat p bands of the calculations. This follows the same procedure as that used with the $E(k_\parallel)$ dispersion data above. Band 4 can then be equated with the upper band of the flat p-band pair. The small curvature in this band is better matched in the LS calculation, as is the dispersion of bands 1 and 7. However, the overall positions of bands in the upper half of the panel are not well reproduced in this calculation; this is another feature of the p-band positioning difficulty already seen in the $E(k_\parallel)$ comparison above.
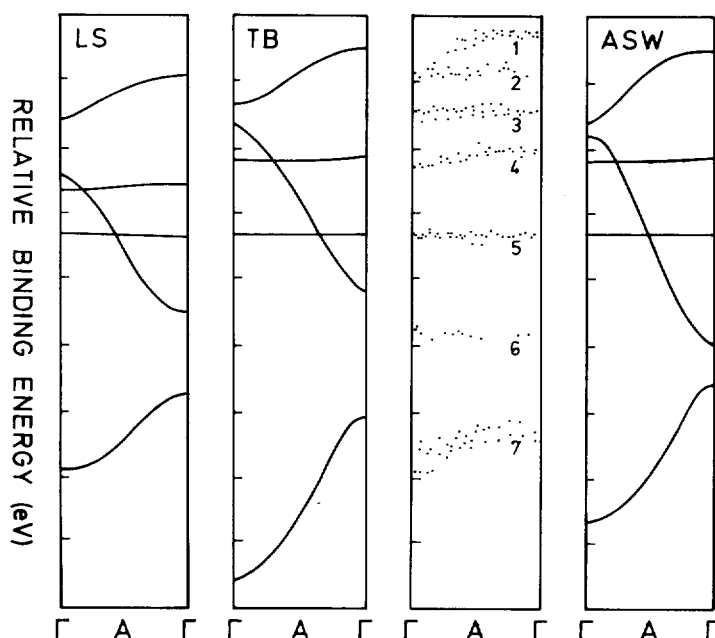

Figure 6. The comparison of the experimental $E(k_\perp)$ dispersion from figure 4(b) with the $\Gamma A \Gamma$ bandstructures from the calculations labelled LS (Doran 1980), TB (Bullett 1978) and ASW (Coehoorn *et al* 1987).

The two calculations with some measure of self-consistency provide a better match in this area, with the TB calculation giving the better estimate of d-band width. Again, this calculation overestimates the overall bandwidth and both the self-consistent calculations overestimate the dispersion in band 7. The large scatter in this p$_z$-like bonding band, which was also seen in the MoSe$_2$ data (Coehoorn *et al* 1987), arises from the poor replication of dispersion in the repeated-zone scheme. This tends to reduce the averaged dispersion in figure 4(b). However, even allowing for this, the experimental dispersion of band 7 is still much lower than these calculations would predict. In general, there is rather less experimental $E(k_\perp)$ dispersion than all the calculations

would indicate. This improves the confidence that can be placed in the comparison of the experimental $E(k_\parallel)$ dispersion with the AL and AH bandstructures as above.

Bands 2, 3 and 6 have no obvious counterparts in the calculations. The band that is predicted to disperse strongly downward with increasing $k_\perp$ is presumably masked by the other emission; it is expected to be weak except at the zone edges. Bands 3 and 6 may be due to density-of-states effects associated with the ends of this strongly dispersing band. Equally, band 2 may be due to density-of-states effects associated with the bottom of the d_{z^2} band. Of these three bands, band 2 is the most persistent throughout the zone and a similar non-dispersing band was reported for $MoSe_2$ (Coehoorn *et al* 1987). That paper suggests polaron bands (de Boer *et al* 1984) or molybdenum impurity states (Eberhardt *et al* 1980) as possible sources of this feature.

5. Conclusions

ARUPS has been applied to determine the electronic bandstructure of the layer-lattice semiconductor molybdenum disulphide, for symmetry directions both parallel and perpendicular to the layers. It is shown that there is reasonable agreement with calculated bandstructures, particularly when the calculation is self-consistent. The experimental $E(k_\parallel)$ dispersion supports the conclusions of recent, related studies and shows how an earlier difficulty with this material arose from mislabelling of symmetry directions. The $E(k_\perp)$ data indicate that dispersion in the ΓA direction is generally less than the calculations predict, which increases the confidence in the $E(k_\parallel)$ analysis.

Acknowledgments

References

Bullett D W 1978 *J. Phys. C: Solid State Phys.* 11 4501
Chiang T-C, Knapp J A, Aono M and Eastman D E 1980 *Phys. Rev.* B 21 3513
Coehoorn R, Haas C, Dijkstra J, Flipse C J F, de Groot R A and Wold A 1987 *Phys. Rev.* B 35 6195
de Boer D K G, van Bruggen C F, Bus G W, Coehoorn R, Haas C,, Sawatzky G A, Myron H W, Norman D and Padmore H M 1984 *Phys. Rev.* B 29 6797
Doran N J 1980 *Physica* B 99 227
Eberhardt W, McGovern I T, Plummer E W and Fischer J E 1980 *Phys. Rev. Lett.* 44 200
Hughes H P and Liang W Y 1973 *J. Phys. C: Solid State Phys.* 6 1684
Lince J R, Didziulis S V and Yarmoff J A 1991 *Phys. Rev.* B 43 4641
Lloyd D R, Quinn C M, Richardson M V and Williams P M 1976 *Commun. Phys.* 1 11
Mamy R, Boufelja A and Carricaburu B 1987 *Phys. Status Solidi* b 141 467
McGovern I T, Williams R H and Parke A W 1979 *J. Phys. C: Solid State Phys.* 12 2689
Mrstik B J, Kaplan R, Reinecke T L, van Hove M and Tong S Y 1977 *Phys. Rev.* B 15 897
Smith N V and Traum M M 1975 *Phys. Rev.* B 11 2087
Williams R H and McEvoy A J 1971 *J. Phys. D: Appl. Phys.* 4 456
Wilson J A and Yoffe A D 1969 *Adv. Phys.* 18 193